

2016
NEW DELHI 5 - 9 DEC. 2016

APMC2016

5 - 9 December 2016, New Delhi, India




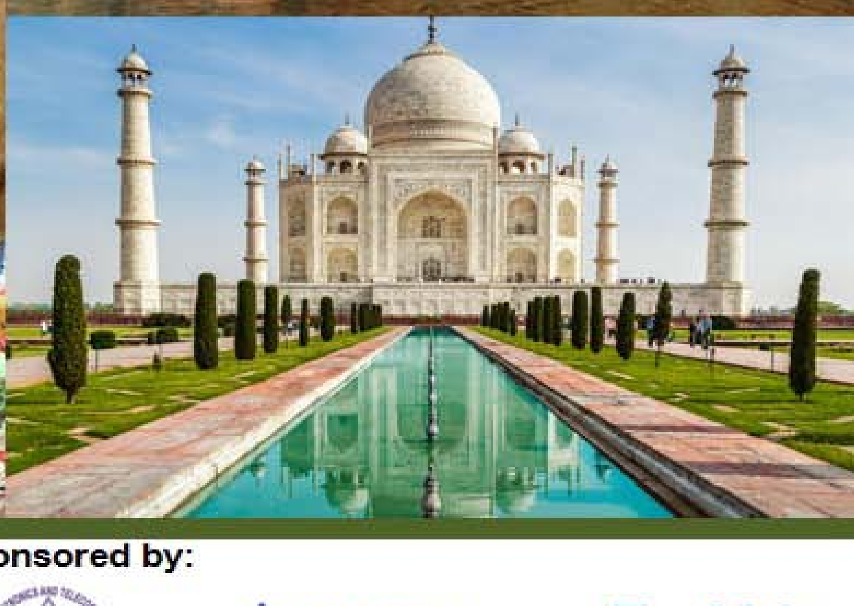

Co-Sponsored by:

IEEE

MTT-S

IEEE Delhi Section

EuMA European Microwave Association

Session: Passive Circuits and Systems
Room: Upper Ground Floor (Next to Exhibition in Peacock Ballroom)
Chair: A. Basu, IIT Delhi
Co-Chairs: M. D. Upadhyay, SNU, Noida

1. WEPA1
A Compact Ultra-wideband Bandpass Filter with High Return Loss Characteristic
P. Kim, G. Chaudhary, Y. Jeong, Chonbuk National University, Jeonju-si, Republic of Korea

2. WEPA2
A comparative study on Explicit and Implicit FDTD methods for Electromagnetic simulation
G. Singh, R. S. Kshetrimayum, T. R. Chanu, NIT Mizoram, Aizawl, India

3. WEPA3
Spoof Surface Plasmon Polaritons (SSPP) Based Multi-Band Bandpass Filter
R. K. Jaiswal, N. P. Pathak, Indian Institute of Technology Roorkee, Roorkee, India

4. WEPA4
Radar Absorbing Structures using Carbon Nano-Composites: EM Design and Performance Analysis
M. CT[1], R. U. Nair[2], H. Singh[2], [1]Cochin University of Science and Technology, Kochi, India, [2]CSIR National Aerospace Laboratories,Bangalore, India

5. WEPA5
High Selectivity Microstrip Bandpass Filter Using Feedback CRLH-TL Unit Cell
A. Alburaikan[1], M. Aqeeli[1], G. N. Jawad[1], A. Biswas [2], Z. Hu[1], [1]University of Manchester, Manchester, United Kingdom, [2]Indian Institute of Technology Kanpur, Kanpur, India

6. WEPA6
Study of Rectangular Open Loop Resonators with Groundings for Low and High Coupling
W. Prasetyo, D. W. Astuti, S. Attamimi, M. Alaydrus, Universitas Mercu Buana, Jakarta, Indonesia

7. WEPA7
A Dual Band Metamaterial Inspired Absorber For WLAN/Wi-MAX Applications Using A Novel I-Shaped Unit Cell Structure
G. Sen, A. Banerjee, M. Kumar, S. N. Islam, S. Das, IIEST, Shibpur, Shibpur, India

8. WEPA8
On the error estimates of the cavity perturbation method
K. Bansal, B. S. Matheru, Solid State Physics Lab,Defence research and development organization, Delhi, India

9. WEPA9
A comparative analysis of hybrid-pol algorithms using RISAT data
A. Kumar[1], R. K. Panigrahi[2], A. Das[3], [1]IIT Roorkee, Roorkee, India, [2]IIT Roorkee, Roorkee, India, [3]ISRO, Ahmedabad, India

10. WEPA10
An exhaustive study of epoxy application in TM mode dielectric Resonator filters
N. Shukla, K. P. Shrivastava, K. V. Trivedi, Space Application Centre, Ahmedabad, India

11. WEPA11
Broadband and High-Purity Ku-Band Circular TE01Mode Converter
J. R. Montejo Garai[1], I. O. Saracho Pantoja[1], J. A. Ruiz Cruz[2], J. M. Rebollar[1], [1]Universidad Politecnica de Madrid, Madrid, Spain,[2]Universidad Autónoma de Madrid, Madrid, Spain

Proceedings of the Asia-Pacific Microwave Conference 2016

A Compact Ultra-wideband Bandpass Filter with High Return Loss Characteristic

Phirun Kim[1], Girdhari Chaudhary[2], and Yongchae Jeong[3]
Division of Electronics and Information Engineering
Chonbuk National University
567 Baekjae-daero, Deokjin-gu, Jeonju-si, Republic of Korea
[1]fmphirun@jbnu.ac.kr
[2]girdharic@jbnu.ac.kr
[3]ycjeong@jbnu.ac.kr

Abstract- **This paper presents a high return loss ultra-wideband bandpass (UWB) filter with a loose coupling of coupled line. A proposed structure consists of shunt short transmission line and a coupled line. By analytically study, a high return loss can be obtained by located a proper five transmission poles in the passband. For an experimental validation, the UWB filter was designed at a center frequency of 6.85 GHz. The measured results agree well with the simulation results. From the measurement, the insertion and return losses were better than 1.5 dB and 20 dB within the operating band from 3 to 11.1 GHz (FBW = 113.2 %).**

Keywords—Coupled line, even-mode, high return loss, odd-mode, ultra wideband bandpass filter.

I. INTRODUCTION

An ultra-wideband (UWB) bandpass filters (BPF) have been developed for use with modern communication systems since early 2002, when the federal communications commission released the frequency band covering 3.1 to 10.6 GHz. Recently, UWB BPFs with different structures have been studied [1-14]. The multiple-mode resonator (MMR) [1]-[5] and the inductance-loaded Y-shaped microstrip resonator [6] were used to design UWB BPFs with a very strong coupling at the external coupling ports. A broadside coupling T-type resonator structure [7] and interdigital coupled lines with an aperture-back [8]-[9] were introduced to improve the coupling by developing the UWB BPF in a multi-layer and microstrip line with sharp selectivity characteristics. In [10], the UWB BPF was analyzed from prototype lumped elements and was implemented using a multilayer liquid-crystal-polymer substrate with eight transmission poles in the passband. In [12], the UWB BPF was designed with several cascaded sections of the transmission line (TL) with short-ended stubs on both the input and output ports. This design did not need coupled resonators. The parallel-coupled microstrip lines with slotted ground below the coupled line were used in [13], and additional capacitors were used to increase the coupling of the coupled line and to provide a high return loss.

This paper investigates a new design structure in order to obtain a high return loss UWB BPF. The proposed structure can provide a high return loss characteristic with a relatively loose coupling of the coupled line and can be fabricated on a microstrip line with a compact size.

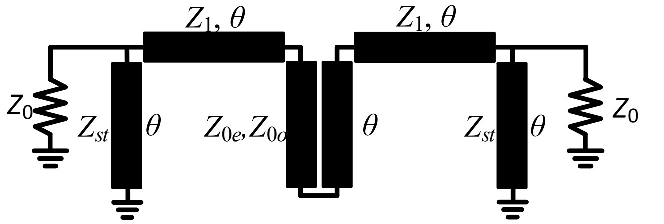

Fig. 1. Structure of the UWB bandpass filter.

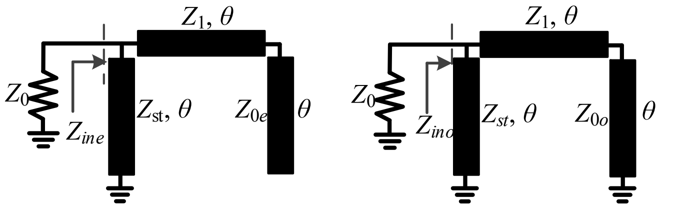

(a) (b)

Fig. 2. Equivalent circuits for the UWB bandpass filter: (a) even-mode and (b) odd-mode.

II. CIRCUIT ANALYSIS

Fig. 1 shows the propose structure of the UWB BPF. The proposed circuit consists of a pair of short-circuited shunt TLs, Z_{st}, and series TLs, Z_1, separated by a shunt coupled TL with characteristic even and odd impedances of Z_{0e} and Z_{0o}. The electrical lengths of all TLs and the coupled line are θ. Since the UWB BPF structure depicted in Fig. 1 is symmetric, even- and odd-mode equivalent circuits are shown in Figs. 2(a) and (b), respectively. Under even- and odd-mode excitations, the symmetrical plane at the center can be considered to be a perfect magnetic wall (open circuit) and electric wall (short circuit), respectively. Then, the even- and odd-mode input impedances can be used to derive the *S*-parameters of the UWB BPF [14] as (1).

$$S_{11} = S_{22} = \frac{Z_{ine}Z_{ino} - Z_0^2}{\left(Z_{ine} + Z_0\right)\left(Z_{ino} + Z_0\right)} \quad (1a)$$

$$S_{21} = S_{12} = \frac{\left(Z_{ine} - Z_{ino}\right) Z_0}{\left(Z_{ine} + Z_0\right)\left(Z_{ino} + Z_0\right)}, \tag{1b}$$

where

$$Z_{ine} = j \frac{Z_{st} Z_1 \left(Z_1 \tan\theta - Z_{0e} \cot\theta\right)}{Z_{st}\left(Z_1 + Z_{0e}\right) + Z_1^2 - Z_1 Z_{0e} \cot^2\theta} \tag{2a}$$

$$Z_{ino} = j \frac{Z_{st} Z_1 \tan\theta \left(Z_{0o} + Z_1\right)}{Z_{st}\left(Z_1 - Z_{0o}\tan^2\theta\right) + Z_1 Z_{0o} + Z_1^2} \tag{2b}$$

$$\theta = \frac{2f}{\pi f_0}. \tag{2c}$$

And the subscripts *e* and *o* denote even- and odd-modes, respectively.

Since the proposed filter consists of five resonators with different characteristic impedances, there are five transmission poles (TPs) can be obtained in the passband. Thus, the locations of the TPs are derived in order to understand the bandwidth effects according to the individual characteristic impedances of the TLs and the coupled line. From (1a), the locations of the TPs are derived as in (3) and (4) by giving $S_{11} = 0$.

$$\cot^2\left(\frac{\pi f}{2 f_0}\right) = 0 \tag{3}$$

$$\frac{f_{pn}}{f_0} = 1 + \left(1 \mp \frac{2}{\pi} \tan^{-1}\sqrt{x}\right), \tag{4}$$

where

$$x = \frac{-a_2 \pm \sqrt{a_2^2 - 4 a_1 a_3}}{2 a_1} \tag{5a}$$

$$a_1 = \left[Z_1^2\left(Z_{0o} + Z_1\right) - Z_{0o} Z_0^2 \left(1 + \frac{Z_{0e}}{Z_1} + \frac{Z_1}{Z_{st}}\right)\right] Z_{st} \tag{5b}$$

$$a_2 = Z_0^2 \left[Z_1\left(Z_{st} + Z_{0o} + 2Z_1 + Z_{0e} + \frac{Z_1 Z_{0o} + Z_1^2}{Z_{st}}\right) + Z_{0e}\left(Z_{st} + 2Z_{0o}\right)\right] - Z_1 Z_{0e} Z_{st}\left(Z_{0o} + Z_1\right) \tag{5c}$$

$$a_3 = \left(1 + \frac{Z_{0o} + Z_1}{Z_{st}}\right) Z_1 Z_{0e} Z_0^2. \tag{5d}$$

From (3), it is evident that one of the TPs always occurred at the center frequency (f_0). Similarly, two pairs of TPs are symmetric with respect to f_0 based on (4) and (5). In order to obtain good UWB passband characteristic, the positions of the TPs should be spaced almost equally.

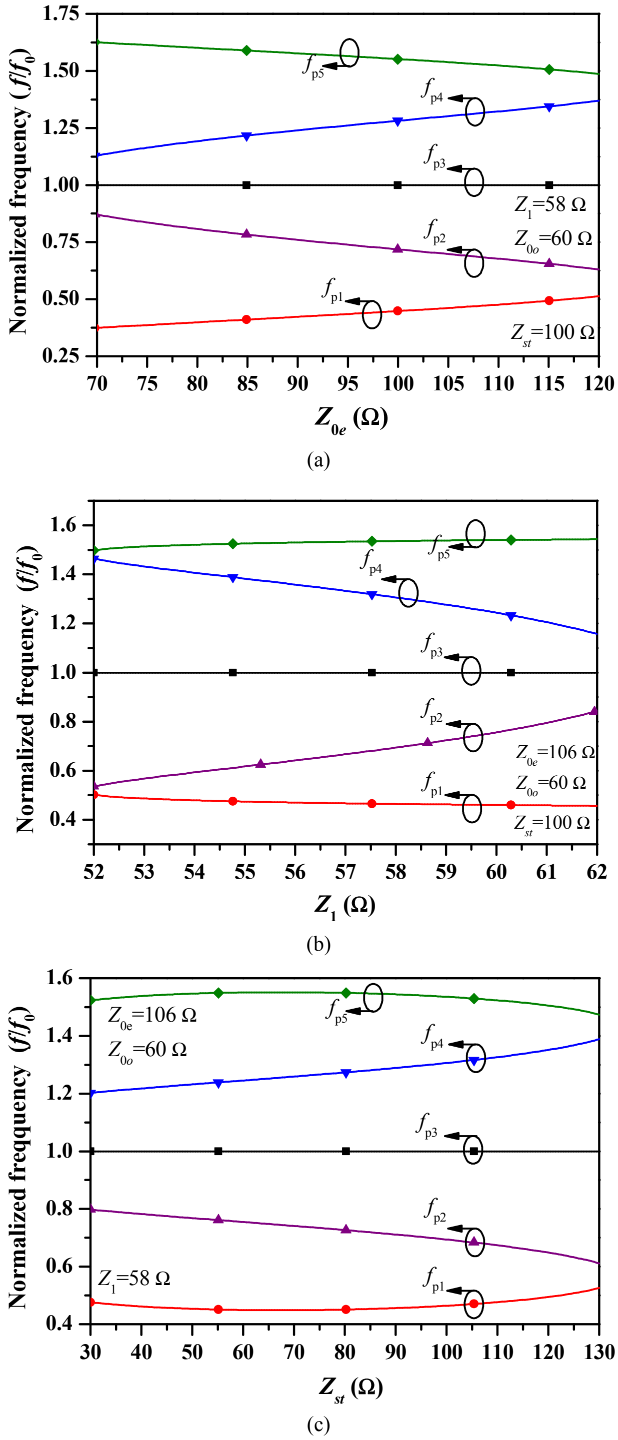

Fig. 3. Transmission pole locations according to: (a) Z_{0e}, (b) Z_1, and (c) Z_{st}.

Figs. 3(a), (b), and (c) show the TP locations according to Z_{0e}, Z_1, and Z_{st}, respectively. As seen in Fig. 3(a), the first and fifth TPs (f_{p1}, f_{p5}) are moved away from the center TP (f_{p3}) as Z_{0e} decreases from 120 Ω to 70 Ω. However, the second and fourth TPs (f_{p2}, f_{p4}) are moved closer to f_{p3}. These calculation assumes Z_{0o} = 60 Ω, Z_1 = 58 Ω, and Z_{st} = 100 Ω. Fig. 3(b) shows f_{p2} and f_{p4} are significantly moved away from f_{p3} as Z_1 decreases. This calculation assumes Z_{0e} = 106 Ω, Z_{0o} = 60 Ω, Z_{st} = 100 Ω, and Z_1 vary from 52 Ω to 62 Ω. On the other hand, f_{p2} and f_{p4} in Fig. 3(c) are moved out from f_{p3}, while f_{p1}

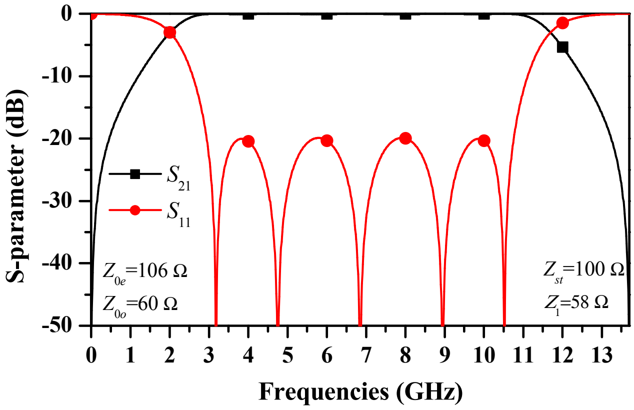

Fig. 4. *S*-parameter characteristics of the UWB bandpass filter.

TABLE I

OPTIMUM TRANSMISSION LINE CHARACTERISTIC IMPEDANCES OF UWB BAND PASS FILTER (UNIT: Ω).

Z_{st}	Z_{0o}	Z_{0e}	Z_1
100	60	106	58

and f_{p5} are tended toward f_{p3} as Z_{st} increases. This calculation assumes Z_{0e} = 106 Ω, Z_{0o} = 60 Ω, Z_1 = 58 Ω, and Z_{st} vary from 30 Ω to 130 Ω. Fig. 3 shows that Z_{0e} and Z_1 have a strong effect on the movement of the TPs. Among the three variables, Z_1 is most sensitive to the TP locations according to the variation. f_{p3} is constant and independent of Z_1, Z_{0e}, and Z_{st}. Since the five TPs can shift within a wide range by changing Z_{0e}, Z_1, and Z_{st}, it is possible to employ a wideband filter to conform to a UWB BPF by choosing appropriate characteristic impedances for the TLs and the couple line. From Fig. 3, the optimum characteristic impedances of transmission line and coupled line are selected and list in Table I. Fig. 4 shows the *S*-parameters of the UWB BPF with equally-spaced TPs in the passband. The fractional bandwidth (FBW) of the 20 dB return loss is obtained 114.1%.

Based on the investigation above, the procedure to design the proposed UWB BPF is summarized in Fig. 5. The design steps for the UWB BPF are as follows.

(a) Specify f_0 and maximum return loss.

(b) Calculate TPs using equations (3) - (4) and then optimize the locations of the TPs.

(c) Calculate the physical dimension of the coupled line and the TLs according to the PCB substrate using microwave circuit or EM simulation software.

(d) Finally, the optimized UWB BPF characteristics are obtained using an EM simulator.

III. SIMULATION AND MEASUREMENT RESULT

An experimental validation was carried out by designing the UWB BPF and fabricating it on an RT 5880 substrate with ε_r = 2.2 and h = 31 mils. An electromagnetic (EM) simulation was

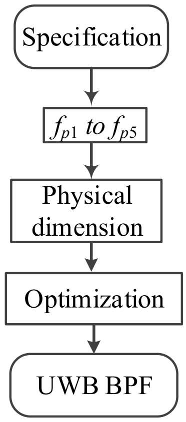

Fig. 5. Design procedure of proposed UWB bandpass filter.

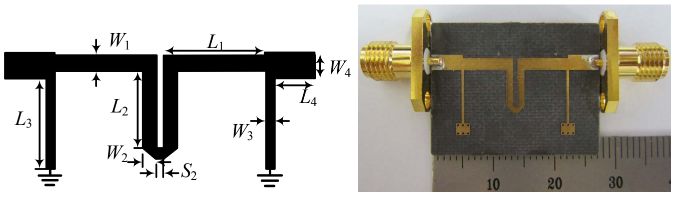

(a) (b)

Fig. 6. (a) Layout and (b) photograph of fabricated the UWB bandpass filter.

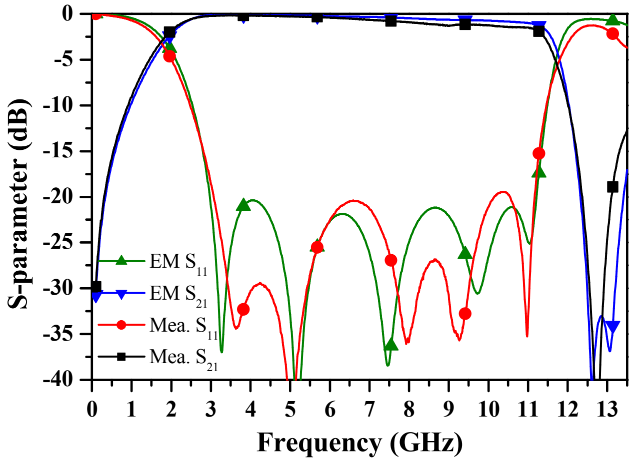

Fig. 7. Simulation and measurement results of the UWB bandpass filter.

TABLE II

PHYSICAL DIMENSIONS OF UWB BANDPASS FILTER (UNIT: MM).

W_1=1.9	W_2=1.1	L_3=8.5
L_1= 8	L_2=5.8	W_4=2.4
S_2=0.7	W_3=0.4	L_4=5

performed using the Ansoft HFSS v15. Based on the design procedure described in the previous section, a UWB BPF was designed and fabricated. From the final optimized values, the physical dimensions were calculated according to the substrate

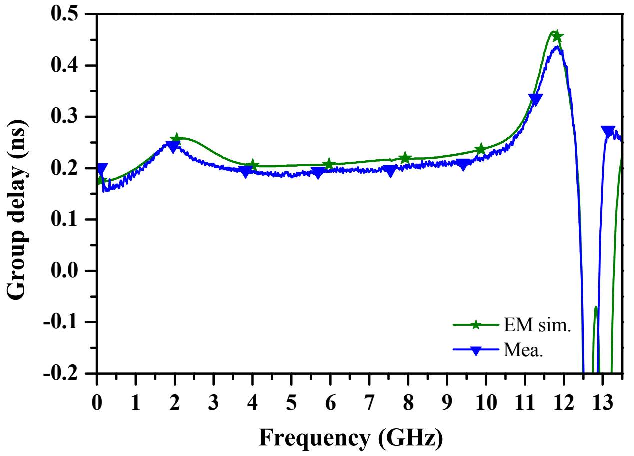

Fig. 8. Simulation and measurement for group delay characteristics of UWB bandpass filter.

using LineCalc of ADS.

Fig. 6 depicts the EM simulation layout and a photograph of the fabricated UWB BPF. The final physical dimensions after a full-wave EM simulation are shown in Table II, and the results of the simulation and measurements of the *S*-parameters and the group delay are shown in Figs. 7 and 8, respectively. The size of the fabricated filter is 12 mm × 18 mm.

The measured results are in good agreement with those obtained from the simulations. As seen in Fig. 7, five TPs were obtained in the passband. The measurements indicate insertion and return losses of 0.59 dB and 20.75 dB at $f_0 = 6.85$ GHz, respectively. Similarly, the FBW for the 20 dB return loss was 113.2% extending from 3.1 GHz to 11.14 GHz. The maximum insertion loss is better than 1.5 dB within the same frequency range. Moreover, the group delay for the filter is 0.24 ± 0.04 ns for the same frequency range.

IV. Conclusion

This paper has demonstrated the design and implementation of high return loss ultra-wideband bandpass filter with a loose coupling of coupled line. The propose structure may be created five transmission poles at the passband. With a loose coupling of coupled line, the propose structure can be implemented on conventional microstrip line. The UWB BPF was designed and measured for verifies the design method. The propose circuit can be obtained a compact size, simple topology, and high return loss.

References

[1] L. Zhu, S. Sun, and W. Menzel, "Ultra-wideband (UWB) bandpass filters using multiple-mode resonator," *IEEE Microw. Wireless Compon. Lett.*, vol. 15, no. 11, pp. 796–798, Nov. 2005.

[2] J. Gao, L. Zhu, W. Menzel, and F. Bögelsack, "Short-circuited CPW multiple-mode resonator for ultra-wideband (UWB) bandpass filter," *IEEE Microw. Wireless Compon. Lett.*, vol. 16, no. 3, pp. 104–106, Mar. 2006.

[3] R. Li and L. Zhu, "Compact UWB bandpass filter using stub-loaded multiple-mode resonator," *IEEE Microw. Wireless Compon. Lett.*, vol. 17, no. 1, pp. 40–42, Jan. 2007.

[4] S. Wong and L. Zhu, "Quadruple-mode UWB bandpass filter with improved out-of-band rejection," *IEEE Microw. Wireless Compon. Lett.*, vol. 19, no. 3, pp. 152–154, Mar. 2009.

[5] Z. Zhang and F. Xiao, "An UWB bandpass filter based on a novel type of multi-mode resonator," *IEEE Microw. Wireless Compon. Lett.*, vol. 22, no. 10, pp. 506–508, Oct. 2012.

[6] K. Song and Q. Xue, "Inductance-loaded Y-shaped resonators and their applications to filters," *IEEE Trans. Microw. Theory Tech.*, vol. 58, no. 4, pp. 978–984, Apr. 2010.

[7] T. Duong and I. Kim, "New elliptic function type UWB BPF bansed on capacitively coupled λ/4 open T resonator," *IEEE Trans. Microw. Theory Tech.*, vol. 57, no. 12, pp. 3089–3098, Dec. 2009.

[8] Q. Chu and X. Tian, "Design of UWB bandpass filter using stepped-impedance stub-loaded resonator," *IEEE Microw. Wireless Compon. Lett.*, vol. 20, no. 9, pp. 501–503, Sep. 2010.

[9] A. Taibi, M. Trabelsi, A. Slimane, M. Belaroussi, and J. Raskin, "A novel design method for compact UWB bandpass filter," *IEEE Microw. Wireless Compon. Lett.*, vol. 25, no. 1, pp. 4–6, Jan. 2015.

[10] Z. Hao and J. Hong, "Ultra-wideband bandpass filter using multilayer liquid-crystal-polymer technology," *IEEE Trans. Microw. Theory Tech.*, vol. 56, no. 9, pp. 2095-2100, Sep. 2008.

[11] R. Zhang and L. Zhu, "Synthesis design of a wideband bandpass filter with inductively coupled short-circuited multi-mode resonator," *IEEE Microw. Wireless Compon. Lett.*, vol. 22, no. 10, pp. 509–511, Oct. 2012.

[12] G. Yang, R. Jin, and J. Geng, "Planar microstrip UWB bandpass filter using U-shaped slot coupling structure," *Electronics Lett.*, vo. 42, no. 25, Dec. 2006.

[13] A. Abbosh, "Design method for ultra-wideband bandpass filter with wide stopband using parallel-coupled microstrip lines," *IEEE Trans. Microw. Theory Tech.*, vol. 60, no. 1, pp. 31-38, Jan. 2012.

[14] L. Zhu, S. Sun, and R. Li, *Microwave Bandpass Filters for Wideband Communications, New York*: Wiley, 2012.